Nonlinear optical coefficients of wurtzite-type α-GaN determined by Raman spectroscopy

Gert Irmer,* Christian Röder, Cameliu Himcinschi, and Jens Kortus
TU Bergakademie Freiberg, Institute of Theoretical Physics, Leipziger Strasse 23, D-09599 Freiberg, Germany
(Received 15 April 2016; revised manuscript received 15 August 2016; published 3 November 2016)

Raman scattering on phonons in GaN with wurtzite structure (α-GaN) is used to determine the coefficients of second-harmonic generation (SHG) and the linear electro-optic effect (LEO) in the region of optical transparency for excitations below the band gap. For wurtzite-type crystals, the symmetry requires that three SHG coefficients d_{31}, d_{33}, and d_{24} and three LEO coefficients r_{31}, r_{33}, and r_{42} be considered. In this work, the dependence of these SHG and LEO coefficients on the Raman scattering intensities of the polar transverse optical (TO) and longitudinal optical (LO) phonon modes in wurtzite-type crystals and their corresponding Faust-Henry coefficients is derived. In the case of GaN, the obtained SHG coefficients are $|d_{31}| = 2.46$ pm/V, $|d_{33}| = 3.97$ pm/V, and $|d_{24}| = 2.48$ pm/V, which agree well with results measured by other methods. Also, all three LEO coefficients of GaN have been determined: $|r_{13}^S| = 0.72$ pm/V, $|r_{33}^S| = 1.31$ pm/V, and $|r_{42}^S| = 0.38$ pm/V. Contrary to previous reports, our results indicate an important contribution of the ionic lattice displacements to the linear electro-optic effect. The ratios of the three SHG coefficients or the three LEO coefficients, which correspond to different nonlinear susceptibility tensor elements, depend on the relative intensities of the polar TO and LO phonon modes connected with different Raman tensor elements.

DOI: 10.1103/PhysRevB.94.195201

I. INTRODUCTION

GaN has attracted considerable interest as material for many electronic and optoelectronic devices with short-wavelength and high-power requirements. Particularly, the consumer electronics segment with light-emitting diode (LED)-based display and LED-based lighting as well as the communication segment with power electronics and switching equipment drive the growth of the global market. The properties of α-GaN make it promising as nonlinear optical material for applications using second-harmonic generation (SHG) or the linear electro-optic effect (LEO). Efficient frequency conversion requires a constant phase relationship among the interacting optical waves over the optical path. In general, the phase-matching condition for the fundamental and second-harmonic wave is not naturally satisfied due to the dispersion of the refractive index. In α-GaN bulk, therefore, the SHG efficiency is too small to be of practical interest [1]. A way to circumvent this is to perform quasiphase matching (QPM) with structures periodically grown with alternating polarities along the optical path. In the case of a one-dimensional (1D) α-GaN photonic crystal, the SHG response was 5000 times greater than for unstructured epilayers [2]. For high-power applications, thicker periodically oriented layers are necessary. Methods have been shown to grow them not on sapphire but on GaN substrates [3]. Because of its large transparency window, α-GaN has the potential as a nonlinear frequency converter in a large frequency range. For orientation-patterned GaAs, it could be already shown to have optical parametric oscillation (OPO) with watt-level output in the mid-IR range [4]. Details of such epitaxially grown structures for QPM applications can be found, for example, in Ref. [5]. The design and analysis of such devices requires accurate values of the linear and nonlinear optical responses. There have been several experimental and theoretical studies for coefficients of the second-harmonic generation (SHG) in α-GaN. In contrast, for the electro-optic effect, there exist only two experimental studies [6,7] with considerable divergences. Shokhovets *et al.* [7] measured it under unclamped conditions and reported only the coefficient r_{31}. In both cases the results were influenced by the piezoelectric effect and acoustic resonances. Long *et al.* [6] measured the coefficients r_{33} and r_{31} and concluded that the linear electro-optic response is predominantly electronic in origin, based on the measured SHG coefficients $\chi_{33}^{(2)} = -20 \pm 6$ pm/V and $\chi_{31}^{(2)} = 10 \pm 3$ pm/V. However, recently measured values of these coefficients are considerably lower (see Table II; d_{33}^E and d_{31}^E correspond to $\chi_{33}^{(2)}/2$ and $\chi_{31}^{(2)}/2$, respectively). Therefore, the assumption of predominantly electronic origin of the LEO coefficient is questionable.

Whereas the first experimental investigations were restricted to thin GaN layers on heterosubstrates, improvements in material quality enable better characterization of the nonlinear optical response. In addition to the conventionally applied methods, Raman scattering can be used to determine the SHG and LEO coefficients below the band gap as shown by Johnston and Kaminow [8]. In binary semiconductors with zincblende structure, one SHG and one LEO coefficient exist; however, for binary semiconductors with wurtzite structure, the symmetry requires three coefficients for each case. In this work, we derive expressions for the six nonlinear optical coefficients as function of the Raman scattering intensity of the polar phonons of A_1 and E_1 symmetry in wurtzite-type crystals and determine them in the case of α-GaN.

II. THEORY

A. Induced nonlinear polarization

The induced polarization in the material can be written as

$$\vec{P} = \varepsilon_0 \chi^{(1)} \vec{E} + \varepsilon_0 \chi^{(2)} \vec{E}^2 + \cdots . \quad (1)$$

In the weak-field approximation, the induced polarization is linearly related to the applied electric field, where ε_0 denotes

*Corresponding author: irmer@physik.tu-freiberg.de

the electric permittivity in vacuum and $\chi^{(1)}$ refers to the susceptibility of the medium. Nonlinearity becomes manifest at higher field amplitudes. The susceptibility coefficients $\chi^{(1)}$ and $\chi^{(2)}$ are tensors of second (i.e., $\chi^{(1)}_{ij}$) and third order (i.e., $\chi^{(2)}_{ijk}$), respectively.

In the case of second-harmonic generation (SHG), also called frequency doubling, two photons of the same frequency ω interact in the nonlinear optical material to generate new photons with frequency 2ω: $\chi^{(2)}(-2\omega;\omega,\omega)$. For the linear electro-optic (LEO) effect, also called the Pockels effect, with $\chi^{(2)}(-\omega;0,\omega)$ the nonlinear response is caused by an electric field with zero or very low frequency. This field induces variation of the refractive index, resulting in a corresponding variation of the intensity or phase of an optical field with frequency ω that is transmitted through or reflected by the electrically activated sample. The frequency ω in the case of constant strain (i.e., clamped case) is well above and in the case of constant stress (i.e., free case) is well below the acoustic resonances of the sample. In comparison with the frequency conversion, no phase-matching requirement between fundamental and generated fields exists as an advantage of the LEO effect, since the frequencies of the two optical waves are identical.

The nonlinear susceptibility tensor $\chi^{(2)}_{ijk}$ is also incorporated in the equations describing the Raman scattering intensity of phonons. The macroscopic electric field that accompanies the polar lattice vibrations provides a source of modulation of the susceptibility of the crystal. The coefficients responsible for the Raman scattering process depend on contributions from the displacements of charged ions and electrons relative to their ionic nuclei. For crystals with wurtzite structure or of higher symmetry, they can be expressed as [9,10]

$$\chi^{(2)}_{ijk} = \frac{\sqrt{\varepsilon_0\varepsilon_{\infty,k}\left(\omega^2_{\mathrm{LO},k}-\omega^2_{\mathrm{TO},k}\right)}}{\omega^2_{\mathrm{TO},k}-\omega^2}\left(\frac{\partial\chi^{(1)}_{ij}}{\partial Q_k}\right)+\left(\frac{\partial\chi^{(1)}_{ij}}{\partial E_k}\right), \quad (2)$$

where k runs from 1 to 3 and denotes the axes x,y,z. $\varepsilon_{\infty,k}$ refers to the high-frequency relative permittivity. The frequencies of the longitudinal (transverse) optical phonon modes are indicated by $\omega_{\mathrm{LO},k}$ ($\omega_{\mathrm{TO},k}$). The ionic and the electronic contribution are related to the susceptibility derivatives with respect to the normal coordinate Q_k and the electric field E_k, respectively. Phonon damping was neglected. For frequencies ω much larger than the phonon frequency $\omega_{\mathrm{TO},k}$, the ionic contribution in Eq. (2) will be very small in comparison with the electronic one. Direct measurements of SHG coefficients have been carried out with exciting light in this frequency range. LEO coefficients have been measured directly with frequencies ω much smaller than the phonon frequencies $\omega_{\mathrm{TO},k}$.

B. Nonlinear optical coefficients

The Raman scattering efficiencies of the polar transverse optical (TO) and longitudinal optical (LO) phonon modes in piezoelectric crystals are correlated with the SHG and LEO coefficients. The so-called nonlinear optical coefficient d^{EO}_{kji} of the Pockels effect for crystals with orthorhombic or higher symmetry, especially with wurtzite structure, where the relative permittivity tensor is diagonal, can be written [9,11] as

$$d^{\mathrm{EO}}_{kji} = d^{I}_{kji} + d^{E}_{kji} = -\varepsilon_{ii}\varepsilon_{jj}r^{S}_{ijk}/4. \quad (3)$$

There are two contributions, where d^{I}_{kji} denote the indirect ones originating from ionic lattice displacements accompanying polar optical phonons and d^{E}_{kji} indicate the pure electronic ones. The so-called electro-optic coefficients of the Pockels effect are denominated by r^{S}_{ijk}. The superscript S refers to the electro-optic coefficients in the case of constant strain (i.e., clamped). The notation of the indices follows Nye [12]. Electro-optic coefficients are measured in the transparent region of the spectrum with photon energies below the band gap. ε_{ii} denotes the relative permittivity at the optical frequency in the direction of the axis i, where i runs from 1 to 3.

The ratios of electronic and ionic contributions are described by the Faust-Henry coefficients C^{FH}_{kji}:

$$C^{\mathrm{FH}}_{kji} = d^{I}_{kji}/d^{E}_{kji}. \quad (4)$$

They can be determined based on the ratio of the measured Raman scattering efficiencies of the TO and LO phonon modes of the appropriate symmetry. The electronic contribution corresponds to the susceptibility derivative with respect to the electric field

$$d^{E}_{kji} = \frac{1}{4}\left(\frac{\partial\chi^{(1)}_{ij}}{\partial E_k}\right) \quad (5)$$

and is connected with the second-harmonic-generation coefficient $d^{\mathrm{SHG}}_{kji} = d^{E}_{kji}$. The ionic contribution is related to the susceptibility derivative with respect to the normal coordinate Q_k and can be expressed as

$$d^{I}_{kji} = \frac{\sqrt{\varepsilon_0\varepsilon_{\infty,k}\left(\omega^2_{\mathrm{LO},k}-\omega^2_{\mathrm{TO},k}\right)}}{4\,\omega^2_{\mathrm{TO},k}}\left(\frac{\partial\chi^{(1)}_{ij}}{\partial Q_k}\right). \quad (6)$$

The derivative of the susceptibility tensor with respect to the normal coordinate Q_k is related to the Raman scattering efficiency [13] of the transverse optical phonon modes.

1. Zincblende structure

At first the introduced formalism is applied in the case of zincblende-type crystals. Binary semiconductors with zincblende structure have one doubly degenerate TO phonon mode and one LO phonon mode at the Γ point of the Brillouin zone. In this case, we have to consider only one SHG and one LEO coefficient, and Eq. (3) reduces to

$$d^{\mathrm{EO}}_{14} = d^{I}_{14} + d^{E}_{14} = (1 + C^{\mathrm{FH}})\,d^{E}_{14} = -\varepsilon^2 r^{S}_{41}/4, \quad (7)$$

where d^{EO}_{14} is the nonlinear optical coefficient of the Pockels effect with the ionic contribution d^{I}_{14} and the electronic contribution d^{E}_{14}. The Faust-Henry coefficient describes their ratio $C^{\mathrm{FH}} = d^{I}_{14}/d^{E}_{14}$ according to Eq. (4). ε indicates the relative permittivity at the optical frequency.

We consider GaAs as a first example. Values for the coefficients r^{S}_{41} and d^{E}_{14} were already calculated from Raman scattering efficiencies by Johnston and Kaminow [8]. Here, we use more recent experimental results in order to verify Eq. (7). Reported values of the LEO coefficient r^{S}_{41} measured with different samples and/or wavelengths below the band gap are

−1.54 and −1.50 pm/V (Ref. [14]), −1.68 and −1.72 pm/V (Ref. [15]), and −1.33, −1.41, −1.46, and −1.53 pm/V (Ref. [16]). Using $r_{41}^S = -1.50$ pm/V, the reported value of the Faust-Henry coefficient $C^{\mathrm{FH}} = -0.51$ (Ref. [16]) measured in the transparent region, and $n = \sqrt{\varepsilon} = 3.38$ we obtain from Eq. (7) $d_{14}^E = 100$ pm/V. This is in the right order of magnitude of several measured values of the SHG coefficient: 100 pm/V (Ref. [17]), 120 pm/V (Ref. [18]), 99 pm/V (Ref. [16]), and 83 pm/V (Ref. [19]) as revised by Roberts [20].

In the case of GaP as a second example with zincblende structure, reported values are $r_{41}^S = -1.1$ pm/V, $n = \sqrt{\varepsilon} = 3.0$ (Ref. [21]), and $C^{\mathrm{FH}} = -0.53$ (Ref. [22]). Using Eq. (7) we obtain $d_{14}^E = 47$ pm/V, which can be compared with experimental values of the SHG coefficient: $d_{14}^{\mathrm{SHG}} = 45$ pm/V (Ref. [19]) and 37 pm/V (Ref. [20]).

2. *Wurtzite structure*

α-GaN with wurtzite structure belongs to the space group C_{6v}^4. $\varepsilon_{11} = \varepsilon_{22} = \varepsilon_\perp$ describes the relative permittivity at the optical frequency in the optically isotropic (x,y) plane and $\varepsilon_{33} = \varepsilon_\parallel$ refers to the relative permittivity in the z direction parallel to the c axis of the uniaxial crystal. The twofold degenerate polar phonon mode with symmetry E_1 vibrates in the (x,y) plane with frequencies $\omega_{\mathrm{TO,E1}}$ and $\omega_{\mathrm{LO,E1}}$. The corresponding normal coordinates are Q_1 and Q_2. Since the phonon mode with symmetry A_1 causes lattice displacements parallel to the z axis with the frequencies $\omega_{\mathrm{TO,A1}}$ and $\omega_{\mathrm{LO,A1}}$, the normal coordinate is Q_3.

According to Claus *et al.* [23] nonzero Raman tensor elements of the transverse optical phonon modes are in the case of α-GaN

$$\begin{aligned} &\frac{\partial\chi_{13}^{(1)}}{\partial Q_1} = \frac{\partial\chi_{31}^{(1)}}{\partial Q_1} = \frac{\partial\chi_{23}^{(1)}}{\partial Q_2} = \frac{\partial\chi_{32}^{(1)}}{\partial Q_2} = c_{\mathrm{TO}}, \\ &\frac{\partial\chi_{11}^{(1)}}{\partial Q_3} = \frac{\partial\chi_{22}^{(1)}}{\partial Q_3} = a_{\mathrm{TO}}, \quad \frac{\partial\chi_{33}^{(1)}}{\partial Q_3} = b_{\mathrm{TO}}. \end{aligned} \tag{8}$$

The absolute values of the three different tensor elements a_{TO}, b_{TO}, and c_{TO} can be determined by measurements of the corresponding Raman scattering efficiencies I_a and I_b of the TO phonon modes with A_1 symmetry and I_c of the TO phonon modes with E_1 symmetry using appropriate scattering geometries as well as polarization configurations. The susceptibility tensor derivative with respect to the normal coordinate Q_k in Eq. (8) should be expressed in units of $\mathrm{kg}^{-1/2}\ \mathrm{m}^{1/2}$.

According to the symmetry, we have to consider three linear electro-optic coefficients r_{13}, r_{33}, r_{42} and three nonlinear SHG coefficients d_{31}, d_{33}, d_{24}. Here, we use the notation introduced by Nye [12] with $r_{113} = r_{13}, r_{333} = r_{33}, r_{232} = r_{42}, d_{311} = d_{31}$, $d_{333} = d_{33}, d_{232} = d_{24}$:

$$\begin{aligned} d_{31}^{EO} &= d_{31}^I + d_{31}^E = \left(1 + C_a^{\mathrm{FH}}\right) d_{31}^E = -\varepsilon_\parallel^2 r_{13}^S/4, \\ d_{33}^{EO} &= d_{33}^I + d_{33}^E = \left(1 + C_b^{\mathrm{FH}}\right) d_{33}^E = -\varepsilon_\perp^2 r_{33}^S/4, \\ d_{24}^{EO} &= d_{24}^I + d_{24}^E = \left(1 + C_c^{\mathrm{FH}}\right) d_{24}^E = -\varepsilon_\parallel \varepsilon_\perp r_{42}^S/4, \end{aligned} \tag{9}$$

where the Faust-Henry coefficients C_a^{FH} and C_b^{FH} are connected with the optical phonon mode of A_1 symmetry and its assigned Raman tensor elements a and b. Accordingly, C_c^{FH} is associated with the phonon mode of E_1 symmetry. Their values were obtained from measured Raman scattering efficiencies of corresponding longitudinal and transverse optical phonon modes which are accessible in appropriate scattering configurations [10].

Using Eqs. (3)–(6), (8), and (9), the nonlinear coefficients can be determined as described by

$$\begin{aligned} d_{31}^I &= \alpha_\parallel a_{\mathrm{TO}}, \quad d_{31}^E = \alpha_\parallel a_{\mathrm{TO}}/C_a^{\mathrm{FH}}, \\ r_{13}^S &= -4\alpha_\parallel a_{\mathrm{TO}}\left(1 + 1/C_a^{\mathrm{FH}}\right)/\varepsilon_\parallel^2, \\ d_{33}^I &= \alpha_\parallel b_{\mathrm{TO}}, \quad d_{33}^E = \alpha_\parallel b_{\mathrm{TO}}/C_b^{\mathrm{FH}}, \\ r_{33}^S &= -4\alpha_\parallel b_{\mathrm{TO}}\left(1 + 1/C_b^{\mathrm{FH}}\right)/\varepsilon_\perp^2, \\ d_{24}^I &= \alpha_\perp c_{\mathrm{TO}}, \quad d_{24}^E = \alpha_\perp c_{\mathrm{TO}}/C_c^{\mathrm{FH}}, \\ r_{42}^S &= -4\alpha_\perp c_{\mathrm{TO}}\left(1 + 1/C_c^{\mathrm{FH}}\right)/\varepsilon_\parallel \varepsilon_\perp, \end{aligned} \tag{10}$$

with the following abbreviations:

$$\begin{aligned} \alpha_\parallel &= \frac{\sqrt{\varepsilon_0 \varepsilon_{\infty,\parallel}\left(\omega_{\mathrm{LO,A1}}^2 - \omega_{\mathrm{TO,A1}}^2\right)}}{4\,\omega_{\mathrm{TO,A1}}^2}, \\ \alpha_\perp &= \frac{\sqrt{\varepsilon_0 \varepsilon_{\infty,\perp}\left(\omega_{\mathrm{LO,E1}}^2 - \omega_{\mathrm{TO,E1}}^2\right)}}{4\,\omega_{\mathrm{TO,E1}}^2}. \end{aligned} \tag{11}$$

Thus, in order to obtain the LEO and SHG coefficients directly from Raman spectroscopic investigations, in addition to the determination of Faust-Henry coefficients, the measurement of the Raman scattering efficiency of the transverse optical Raman modes is necessary. This will be shown in Sec. III.

III. EXPERIMENTAL RESULTS

A. Raman scattering efficiencies

The determination of the nonlinear optical coefficients of α-GaN using Eq. (10) requires data of Raman tensor elements a_{TO}, b_{TO}, and c_{TO} and corresponding Faust-Henry coefficients C_a^{FH}, C_b^{FH}, and C_c^{FH}. In this work, we use values published by Irmer *et al.* [10]. The Raman tensor elements given therein are normalized with respect to that of the strong nonpolar $E_{2,\mathrm{high}}$ phonon at 567.6 cm^{-1} which was set $d = 1$. For the measurements, scattering configurations were realized, in such a way that both (i) TO phonons or LO phonons and (ii) the $E_{2,\mathrm{high}}$ Raman mode as an inner standard were allowed. As an example in Fig. 1 Raman spectra recorded in backscattering geometry are shown.

From these data, the relative intensities of the $\mathrm{TO}_{\mathrm{A1},a}$ and $\mathrm{LO}_{\mathrm{A1},a}$ phonon modes were deduced. Backscattering measurements can also be used to ascertain the relative intensities of $\mathrm{TO}_{\mathrm{A1},b}$ and $\mathrm{TO}_{\mathrm{E1},c}$ phonon modes. The intensity ratio of the $\mathrm{LO}_{\mathrm{E1},c}$ and $\mathrm{TO}_{\mathrm{E1},c}$ phonons is accessible in 90° scattering geometry. The determination of the $\mathrm{LO}_{\mathrm{A1},b}$ to $\mathrm{TO}_{\mathrm{A1},a}$ intensity ratio requires near 0° scattering geometry. For more details we refer to our previous work [10]. The relative Raman tensor elements which were deduced from the relative intensities are included in Table I.

However, the Raman tensor elements a_{TO}, b_{TO}, and c_{TO} included in Eq. (10) are absolute values. Therefore, we

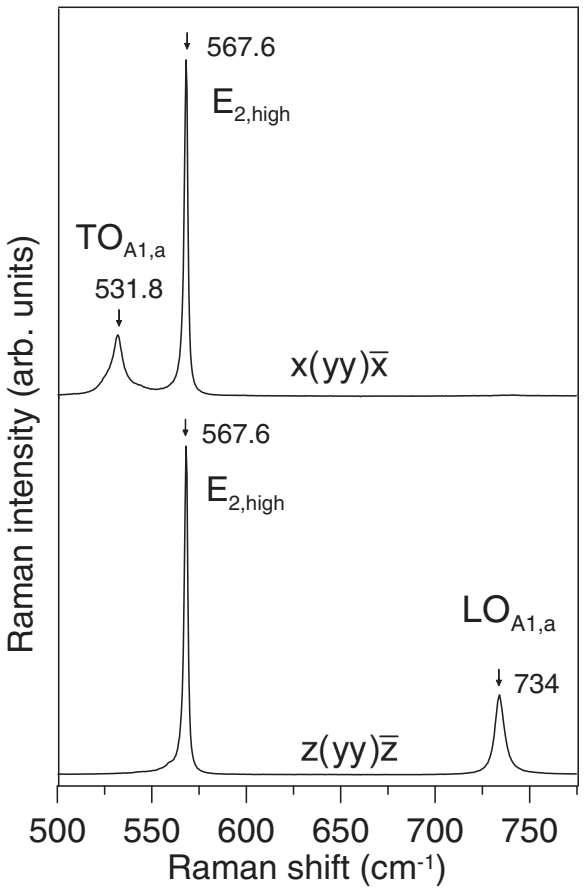

FIG. 1. Normalized Raman spectra with respect to the intensity of the $E_{2,\mathrm{high}}$ Raman mode and the observable TO and LO phonon modes of A_1 symmetry, which are connected with the Raman tensor elements a_{TO} and a_{LO}. The spectra were excited with the 514.5-nm line of an Ar^+ laser and recorded in backscattering geometry at room temperature. The polarization configurations $x(yy)\bar{x}$ and $z(yy)\bar{z}$ according to Porto's notation [24] were realized.

determined the absolute Raman efficiency of the $E_{2,\mathrm{high}}$ phonon on the same crystal as used in Ref. [10]. The connection of the Raman scattering efficiency of the nonpolar twofold degenerate E_2 phonon mode with its assigned Raman tensor elements is given by

$$I_{\mathrm{E2}} = \frac{\partial S_{\mathrm{E2}}}{\partial \Omega} = \frac{\omega_{\mathrm{S,E2}}^4 \hbar (n_{\mathrm{E2}}+1)}{32\pi^2 c^4 \omega_{\mathrm{E2}}} \cdot \frac{\omega_{\mathrm{L}}}{\omega_{\mathrm{S,E2}}} \sum_{i=1,2} |\vec{e}_{\mathrm{S}} \cdot \tilde{R}_{\mathrm{E2},i} \cdot \vec{e}_{\mathrm{L}}|^2. \tag{12}$$

In this equation I_{E2} indicates the Raman scattering efficiency in units of $\mathrm{m^{-1}\ sr^{-1}}$ as the ratio of scattered to incident power per unit solid angle Ω and scattering length path. Its relation to the differential Raman cross section $\partial\sigma/\partial\Omega$ is $\partial S/\partial\Omega = (1/V)\,\partial\sigma/\partial\Omega$, where V denotes the effective scattering volume [13]. ω_{L} and $\omega_{\mathrm{S,E2}}$ refer to the frequencies of the exciting laser light and the scattered light, respectively. $n_{\mathrm{E2}} = 1/[\exp(\hbar\omega_{\mathrm{E2}}/kT) - 1]$ is the Bose-Einstein factor. The factor $\omega_{\mathrm{L}}/\omega_{\mathrm{S,E2}}$ takes into account the registration of the Raman spectrum by means of photon counting. The polarizations of the incident and scattered light are described by the unit vectors $\vec{e}_{\mathrm{L}}$ and $\vec{e}_{\mathrm{S}}$. According to Claus *et al.* [23] nonzero Raman tensor elements are $(R_{\mathrm{E2},1})_{12} = (R_{\mathrm{E2},1})_{21} = -d$, $(R_{\mathrm{E2},2})_{11} = d$, $(R_{\mathrm{E2},2})_{22} = -d$.

The absolute Raman scattering efficiency of the $E_{2,\mathrm{high}}$ Raman mode was determined by the external standard method where intensities of sample and reference standard are recorded consecutively under identical conditions. As reference standard we have chosen CCl_4 where absolute scattering efficiencies are available in literature.

The Raman spectra were recorded in the macro chamber of a T64000 Raman spectrometer from Horiba/Jobin Yvon in 90° scattering geometry. The spectra were excited with the 514.5-nm line of an Ar^+ laser at power level of about 50 mW before the sample. The scattering configuration is shown in Fig. 2. The exciting linearly polarized laser beam focused by a laser objective is directed along the x axis of the laboratory coordinate system and enters the surface of the prismatic sample or the prismatic liquid cell. The scattered light falls within the solid angle ϑ onto the entrance lens. It should be noted that due to the refraction of the scattered light at the boundary of sample-air the effective solid angle $\vartheta_{\mathrm{sample}}$ for scattered light passing the entrance lens is smaller inside the sample. This fact is depicted in more detail in the upper part of Fig. 2. Then, the scattered light originating from the focus plane of the entrance lens passes an analyzer and a quartz wave plate which rotates the polarization axis in the

TABLE I. Scattering cross sections and Raman tensor elements of the $E_{2,\mathrm{high}}$ Raman mode and the polar phonon modes of α-GaN. The errors of the adapted relative values [10] amounts to about 3%; the error of the absolute values is about 20%.

Raman mode	Raman shift ($\mathrm{cm^{-1}}$)	Scattering cross section		Raman tensor element	
		Relative	Absolute ($10^{-5}\mathrm{m^{-1}\ sr^{-1}}$)	Relative	Absolute ($10^8\ \mathrm{kg^{-1/2}\ m^{1/2}}$)
$E_{2,\mathrm{high}}$	567.6	1	3.2	$d^2 = 1$	$\lvert d\rvert = 6.86$
$\mathrm{TO}_{\mathrm{A1},a}$	531.8	0.63	2.02	$a_{\mathrm{TO}}^2/d^2 = 0.58$	$\lvert a_{\mathrm{TO}}\rvert = 5.23$
$\mathrm{LO}_{\mathrm{A1},a}$	734	0.66	2.11	$a_{\mathrm{LO}}^2/d^2 = 0.92$	$\lvert a_{\mathrm{LO}}\rvert = 6.58$
$\mathrm{TO}_{\mathrm{A1},b}$	531.8	1.98	6.34	$b_{\mathrm{TO}}^2/d^2 = 1.82$	$\lvert b_{\mathrm{TO}}\rvert = 9.26$
$\mathrm{LO}_{\mathrm{A1},b}$	734	2.00	6.40	$b_{\mathrm{LO}}^2/d^2 = 2.78$	$\lvert b_{\mathrm{LO}}\rvert = 11.44$
$\mathrm{TO}_{\mathrm{E1},c}$	558.8	0.35	1.12	$c_{\mathrm{TO}}^2/d^2 = 0.34$	$\lvert c_{\mathrm{TO}}\rvert = 4.00$
$\mathrm{LO}_{\mathrm{E1},c}$	741	0.43	1.38	$c_{\mathrm{LO}}^2/d^2 = 0.61$	$\lvert c_{\mathrm{LO}}\rvert = 5.36$

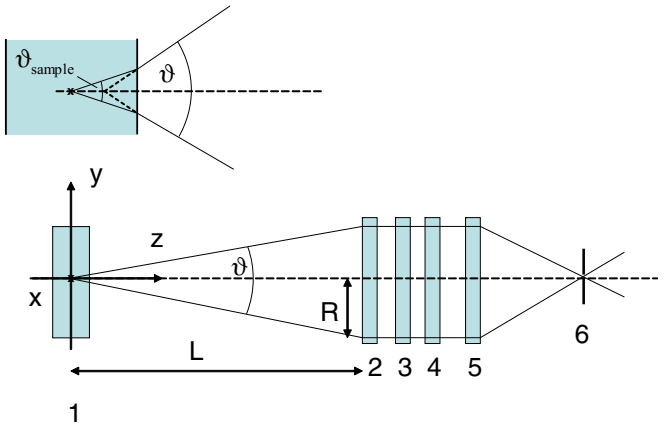

FIG. 2. 90° scattering configuration for the determination of the absolute Raman scattering efficiency. The exciting laser beam was directed along the x axis of the laboratory coordinate system. (1) GaN crystal or prismatic liquid cell, (2) entrance lens, (3) analyzer, (4) quartz plate, rotatable (5) lens, and (6) spectrometer entrance slit. Due to the refraction of the scattered light at the boundary of sample-air, the effective solid angle $\vartheta_{\text{sample}}$ for scattered light passing the entrance lens is smaller inside the sample (upper part).

position for which the spectrometer throughput is optimized. After passing the monochromator in subtractive mode, the scattered light was detected by a charge coupled device (CCD). The sample holder was covered with a mask permitting only light scattered from the central position of the sample or cell to pass onto the spectrometer so that reflected and other stray light have been effectively excluded. Corrections were made for the reflectivity of the crystal and the liquid to both the incident and the scattered light. The length of the effective light path entering the spectrometer was controlled with masks in the plane of the entrance slits and could be observed with a periscope.

The dimensions of the α-GaN single crystal were about $5 \times 5 \times 1$ mm. The GaN crystal was grown by hydride vapor phase epitaxy (HVPE) along the c axis. In our setup, its c axis is oriented parallel to the z axis of the laboratory coordinate system. In Fig. 3 room-temperature Raman spectra recorded in 90° scattering geometry as indicated by the notation $x(yy)z$ and $x(yx)z$ are shown. In both polarization configurations, the Raman intensity of the $E_{2,\text{high}}$ phonon mode proportional to $\sum_{i=1,2} |\vec{e}_S \cdot \tilde{R}_{E2,i} \cdot \vec{e}_L|^2 = d^2$ is obtained (see Fig. 3).

Using 90° scattering geometry the transferred phonon wave vector includes an angle of $\theta = 45°$ to the optical c axis of the crystal. Whereas symmetry and frequency of the nonpolar $E_{2,\text{high}}$ Raman mode are not influenced by the angle θ, for the polar TO and LO phonon modes directional dispersion occurs as indicated by the inset of Fig. 3 in the case of the TO branches. For $\theta = 0°$ polar phonon modes are observed at $\omega_{\text{LO,A1}} = 734$ cm^{-1} and at $\omega_{\text{TO,E1}} = 558.8$ cm^{-1} with the wave vector parallel to the c axis. In the case of $\theta = 90°$ with the transferred wave vector lying in the optically isotropic (x,y) plane the phonon frequencies $\omega_{\text{LO,E1}} = 741$ cm^{-1}, $\omega_{\text{TO,A1}} = 531.8$ cm^{-1}, and $\omega_{\text{TO,E1}} = 558.8$ cm^{-1} are observable [25]. In the limit of $\theta = 0°$ and $\theta = 90°$, the polar phonon modes have defined symmetry A_1 or E_1. This is not the case for intermediate angles

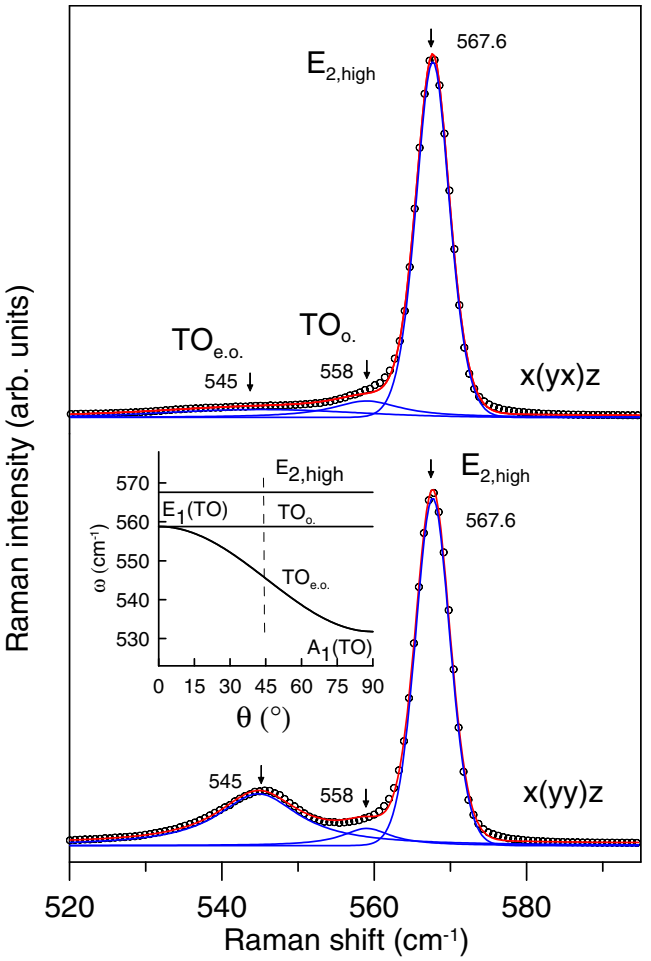

FIG. 3. Raman spectra of the $E_{2,\text{high}}$ phonon mode recorded in scattering configurations $x(yy)z$ and $x(yx)z$. The inset shows the frequency dependence of the extraordinary TO phonon mode ($\text{TO}_{\text{e.o.}}$) on the angle θ between the transferred wave vector and the c axis of the crystal.

θ for the extraordinary branches (i.e., $\text{TO}_{\text{e.o.}}$ and $\text{LO}_{\text{e.o.}}$) whose frequencies are changed continuously according to $A_1(\text{LO}) \rightarrow E_1(\text{LO})$ and $E_1(\text{TO}) \rightarrow A_1(\text{TO})$ while the LO or TO character is maintained. For the third polar mode, the ordinary one (i.e., $\text{TO}_{\text{o.}}$), $E_1(\text{TO}) \rightarrow E_1(\text{TO})$ is observed and the frequency does not depend on the angle θ.

The area of the $E_{2,\text{high}}$ phonon peak was ascertained in each Raman spectrum by deconvolution of the spectra using Gaussian-Lorentzian mixed functions for the $E_{2,\text{high}}$ phonon, the extraordinary TO phonon at 545 cm^{-1}, and the ordinary $E_1(\text{TO})$ phonon at 558.8 cm^{-1} (see Fig. 3). In the case of CCl_4 we decided to analyze the Raman intensity of the totally polarized band at 459 cm^{-1} which is close to the wave number of the $E_{2,\text{high}}$ phonon mode. Thus, the influence of the spectral dependence of the spectrometer and detector was minimized. The reported absolute Raman scattering efficiency $I_{459}^{CCl_4} = 1.10 \times 10^{-5}$ m^{-1} sr^{-1} was taken from Ref. [26].

Comparing both, the area of the $E_{2,\text{high}}$ phonon peak and that one of the CCl_4 Raman band at 459 cm^{-1}, we obtained the scattering efficiency of the α-GaN crystal

TABLE II. Second-harmonic-generation (SHG) coefficients of α-GaN.

	$\lvert d_{31}^E \rvert$ (pm/V)	$\lvert d_{33}^E \rvert$ (pm/V)	$\lvert d_{24}^E \rvert$ (pm/V)	Sample thickness
This work	2.46	3.97	2.48	800 μm
Sanford	2.65	4.0		160.14 μm, free standing
et al. [31]	2.75	4.6		229.67 μm, free standing
Miragliotta	2.40	4.795	2.40	5.31 μm
et al. [1]	2.205	4.48	2.24	3.00 μm
	2.165	4.165	2.08	2.25 μm
Kravetsky	2.73	5.64	2.74	1 μm
et al. [32][a]				

[a]The values reported in Ref. [32] have been divided by factor 2 in order to adapt them to the introduced definitions used here.

for the $E_{2,\text{high}}$ phonon mode as $I_{\text{E2}} = I_{567}^{\text{GaN}} = (3.2 \pm 0.7) \times 10^{-5}$ m^{-1} sr^{-1}. Based on this value, the absolute Raman scattering efficiencies for α-GaN have been calculated and are summarized in Table I. Their estimated error amounts to about 20%.

B. Nonlinear optical coefficients

According to Eq. (10) the determination of the nonlinear optical coefficients of α-GaN requires data of Raman tensor elements a_{TO}, b_{TO}, c_{TO} and corresponding Faust-Henry coefficients C_a^{FH}, C_b^{FH}, C_c^{FH}. With the above determined absolute Raman scattering efficiency of the $E_{2,\text{high}}$ Raman mode the magnitude of the corresponding Raman tensor element was calculated according to Eq. (12): $d = 6.86 \times 10^8$ kg$^{-1/2}$ m$^{1/2}$. Subsequently, the absolute values of the remaining Raman tensor elements were obtained (see last column of Table I) [27]

The estimated error of the absolute values amounts to about 20%, and the error of the relative Raman tensor elements in Table I is about 3%. The Faust-Henry coefficients can be expressed in dependence on the relative Raman tensor elements [see Ref. [10], Eq. (10)]. Therefore, the Raman tensor elements of corresponding TO and LO phonon modes are listed in Table I. The obtained set of Faust-Henry coefficients was adopted from Irmer *et al.* [10]: $C_a^{\text{FH}} = -3.46$, $C_b^{\text{FH}} = -3.81$, and $C_c^{\text{FH}} = -2.31$.

The anisotropy of the relative permittivity of α-GaN is small [28–30]. At the frequency of the scattered light excited with the laser wavelength 514.5 nm, the value $\varepsilon_\parallel = \varepsilon_\perp \approx 5.83$ was utilized [30]. As the high-frequency permittivity, the value $\varepsilon_{\infty\parallel} \approx \varepsilon_{\infty\perp} = 5.37$ calculated [30] from the first-order Sellmeier equation for $\lambda \to \infty$ was used, which is in good agreement with the value 5.35 measured by Barker *et al.* [28].

Table II shows our results in comparison with other experimental results. The review by Miragliotta and Wickenden [1] also contains older results, which deviate considerably from the newer ones. We are aware of only one other experimental determination under clamped conditions of the LEO coefficients in α-GaN; see Table III. The value $r_{13} = (1.55 \pm 0.08)$ pm/V measured by electroreflectance with unclamped experiment was reported by Shokhovets *et al.* [7].

TABLE III. Linear electro-optic (LEO) coefficients of α-GaN.

	$\lvert r_{13}^S \rvert$ (pm/V)	$\lvert r_{33}^S \rvert$ (pm/V)	$\lvert r_{42}^S \rvert$ (pm/V)	Sample thickness
This work	0.72	1.31	0.38	800 μm
Long *et al.* [6]	0.57 ± 0.11	1.91 ± 0.35		4.62 μm

IV. DISCUSSION

The susceptibility derivatives depend, in general, on frequency and do not have the same magnitude for measurements of the second-harmonic generation, Raman scattering cross section, and electro-optic effect. However, the frequency dependence is small in the range of optical transparency well below the electronic transitions of the crystal [9].

The determination of absolute values of the LEO and SHG coefficients from Raman scattering measurements requires absolute values of the Raman scattering efficiencies, which cannot be easily obtained and are a source of errors. Only one other measurement on α-GaN is known to us. Loa *et al.* [33] measured the Raman scattering efficiencies of α-GaN layers in backscattering geometry. Using their value $(3.8 \pm 1.1) \times 10^{-5}$ m^{-1} sr^{-1} (Ref. [33]) for the Raman efficiency of the $E_{2,\text{high}}$ phonon instead of our result $(3.2 \pm 0.7) \times 10^{-5}$ m^{-1} sr^{-1} would result in 9% greater coefficients in Tables II and III. However, Eqs. (10) show that the ratios between the three coefficients SHG and LEO, respectively, depend only on ratios of the intensities of the TO phonons and of the Faust-Henry coefficients of different symmetry, which can be accurately determined by Raman measurements with suitable scattering geometry. The factors $\alpha_\parallel$ and $\alpha_\perp$ defined in Eq. (11) are precisely known. Therefore, the error of the coefficient ratios is mainly caused by errors of the square root of intensity ratios and should be in the order of a few percent.

The signs of the nonlinear optical coefficients are often given controversially in the literature. Unfortunately, they cannot be determined with measurements of the Raman efficiency due to its quadratic dependence on the tensor elements [see Eq. (12)]. However, some constraints exist. With the applied Faust-Henry coefficients $C_a^{\text{FH}} = -3.46$, $C_b^{\text{FH}} = -3.81$, and $C_c^{\text{FH}} = -2.31$, we obtain from Eq. (9) the correlations $d_{31}^E/r_{13}^S > 0$, $d_{33}^E/r_{33}^S > 0$, and $d_{24}^E/r_{42}^S > 0$. For some geometrical configurations of Raman measurements the efficiencies depend on sums or differences of a_{TO} and b_{TO} (see Table I in Ref. [10]). From comparison of these efficiencies it is possible to conclude that $a_{\text{TO}}/b_{\text{TO}} < 0$ and therefore $d_{33}^I/d_{31}^I < 0$, $d_{33}^E/d_{31}^E < 0$, and $r_{33}^S/r_{13}^S < 0$.

For an ideal hexagonal wurtzite structure, the nonzero tensor elements of the SHG tensor are not independent and related by the following expressions: $d_{31} = d_{24}$, $d_{31} = -d_{33}/2$ [31,34], derived by arguments based on symmetry considerations. Whereas the first expression is well satisfied by our results, the second one is not rigorously verified (see Table II). A reason could be that this constraint is based on the premise that the optical nonlinearity in the hexagonal structure is due entirely to the contributions of tetrahedral units [31,34].

Our results have a considerable ionic part of the electro-optic coefficient: $|r_{33}^I| = 4|d_{33}^I|/\varepsilon_\perp^2 = 1.78$ pm/V and

$|r^I_{13}| = 4|d^I_{31}|/\varepsilon^2_{\parallel} = 1.00$ pm/V. We can compare these results with theoretical values based on the bond-charge dielectric theory of Phillips and Van Vechten. We used the equations given by Shih and Yariv [35,36] with parameters of α-GaN calculated by Van Vechten [37] and obtain $|r^I_{33}| = 1.43$ pm/V and $|r^I_{13}| = |r^I_{33}|/2 = 0.72$ pm/V, respectively.

From Raman scattering efficiencies of corresponding TO and LO phonon modes the Faust-Henry coefficients can be deduced. However, for each coefficient two possible solutions can be found. We applied here the set of Faust-Henry coefficients for α-GaN which was unambiguously in accordance with results of near-forward scattering of phonon-polaritons [10,38]. Using the second set of coefficients $C^{\mathrm{FH}}_a = 0.40$, $C^{\mathrm{FH}}_b = 0.40$, and $C^{\mathrm{FH}}_c = 0.33$ the following nonlinear coefficients have been obtained: $|d^E_{31}| = 21.4$, $|d^E_{33}| = 37.8$, $|d^E_{24}| = 17.3$, $|r^S_{13}| = 3.5$, $|r^S_{33}| = 6.2$, and $|r^S_{42}| = 2.7$ pm/V. The comparison of these values with experimental results in Tables II and III shows that the second set of Faust-Henry coefficients can be excluded due to the very large differences of the calculated values and experimental SHG and LEO coefficients.

V. CONCLUSION

The determination of the SHG and LEO coefficients of nonlinear optical materials with conventional methods is not simple and often has deviating results. This applies also to the technically important semiconductor α-GaN with partially incomplete and controversially reported data. For the range of optical transparency below the band-gap measurements of the Raman scattering intensity of phonons can be used for the determination of the coefficients. This is shown for crystals with wurtzite structure. For relations between the coefficients corresponding to different tensor elements it is sufficient to compare the relative intensity ratios of the polar phonons with different symmetry. The three SHG coefficients of α-GaN determined with Raman spectroscopy agree well with recent results obtained by other experimental methods. Additionally, all three LEO coefficients have been determined, including the coefficient $|r^S_{42}|$. Our results clearly indicate, contrary to previous reports, an important contribution of the ionic lattice displacements to the LEO effect.

ACKNOWLEDGMENTS

The authors gratefully acknowledge the fruitful cooperation with G. Leibiger and F. Habel (Freiberger Compound Materials GmbH), especially in providing high-quality GaN specimens as well as supporting the sample preparation. This work was financially supported by the European Union (European Social Fund) and by the Saxonian Government (Grant No. 100231954).

[1] J. A. Miragliotta and D. K. Wickenden, *Gallium Nitride (GaN) II*, Semiconductors and Semimetals Vol. 57 (Academic Press, San Diego, CA, 1999), pp. 319–369.
[2] J. Torres, D. Coquillat, R. Legros, J. P. Lascaray, S. Ruffenach, O. Briot, R. L. Aulombard, D. Peyrade, Y. Chen, M. Le Vassor d'Yerville, E. Centeno, D. Cassagne, and J. P. Albert, Phys. Status Solidi B **240**, 455 (2003).
[3] J. Hite, M. Twigg, M. Mastro, J. Freitas Jr., J. Meyer, I. Vurgaftman, S. O'Connor, N. Condon, F. Kub, S. Bowman, and C. Eddy Jr., Opt. Mater. Express **2**, 1203 (2012).
[4] C. Kieleck, A. Hildenbrand, M. Eichhorn, D. Faye, E. Lallier, B. Grard, and S. D. Jackson, Proc. SPIE **7836**, 783607 (2010).
[5] A. C. Lin, Ph.D. thesis, Stanford University, 2012.
[6] X.-C. Long, R. A. Myers, S. R. J. Brueck, R. Ramer, K. Zheng, and S. D. Hersee, Appl. Phys. Lett. **67**, 1349 (1995).
[7] S. Shokhovets, R. Goldhahn, and G. Gobsch, Mater. Sci. Eng. B **93**, 215 (2002).
[8] W. D. Johnston Jr. and I. P. Kaminow, Phys. Rev. **188**, 1209 (1969).
[9] W. Hayes and R. Loudon, *Scattering of Light by Crystals* (Dover Publications, Mineola, NY, 2004).
[10] G. Irmer, C. Röder, C. Himcinschi, and J. Kortus, J. Appl. Phys. **116**, 245702 (2014).
[11] W. D. Johnston Jr., Phys. Rev. B **1**, 3494 (1970).
[12] J. F. Nye, *Physical Properties of Crystals: Their Representation by Tensors and Matrices* (Oxford Science Publications, Oxford, UK, 2002).
[13] M. Cardona, *Light Scattering in Solids II* (Springer-Verlag, Berlin, 1982), p. 19.
[14] C.-A. Berseth, C. Wuethrich, and F. K. Reinhart, J. Appl. Phys. **71**, 2821 (1992).
[15] J. Faist and F.-K. Reinhart, J. Appl. Phys. **67**, 7006 (1990).
[16] N. Suzuki and K. Tada, Jpn. J. Appl. Phys. **23**, 1011 (1984).
[17] S. Bergfeld and W. Daum, Phys. Rev. Lett. **90**, 036801 (2003).
[18] A. Fiore, V. Berger, E. Rosencher, P. Bravetti, and J. Nagle, Nature (London) **391**, 463 (1998).
[19] B. F. Levine and C. G. Bethea, Appl. Phys. Lett. **20**, 272 (1972).
[20] D. A. Roberts, IEEE J. Quantum Electron. **28**, 2057 (1992).
[21] S. Adachi and K. Oe, J. Appl. Phys. **56**, 74 (1984).
[22] G. Irmer, V. V. Toporov, B. H. Bairamov, and J. Monecke, Phys. Status Solidi B **119**, 595 (1983).
[23] R. Claus, L. Merten, and J. Brandmüller, *Light Scattering by Phonon-Polaritons*, edited by G. Höhler (Springer-Verlag, Berlin, 1975).
[24] T. C. Damen, S. P. S. Porto, and B. Tell, Phys. Rev. **142**, 570 (1966).
[25] V. Y. Davydov, Y. E. Kitaev, I. N. Goncharuk, A. N. Smirnov, J. Graul, O. Semchinova, D. Uffmann, M. B. Smirnov, A. P. Mirgorodsky, and R. A. Evarestov, Phys. Rev. B **58**, 12899 (1998).
[26] Y. Kato and H. Takuma, J. Chem. Phys. **54**, 5398 (1971).
[27] In order to give the tensor elements in units of area, expressed in $\mathrm{Å}^2$, the conversion $a(10^{20}/4\pi)(m_{\mathrm{red}}/N_{\mathrm{pc}})^{1/2}$ can be used. In this formula, the tensor element a is given in units of $\mathrm{kg}^{-1/2}\mathrm{m}^{1/2}$, m_{red} refers to the reduced mass of the vibrating atoms of the two sublattices expressed in kg, and N_{pc} indicates the number of primitive cells per unit volume expressed in

m^{-3}. In the case of α-GaN the corresponding values are as follows: $N_{pc} = 2.186 \times 10^{28}$ m^{-3}, for the $E_{2,high}$ phonon mode $m_{red} = m_N/2 = 1.163 \times 10^{-26}$ kg, and for the TO phonon modes $m_{red} = (m_{Ga}m_N)/(m_{Ga} + m_N) = 1.937 \times 10^{-26}$ kg.

[28] A. S. Barker Jr. and M. Ilegems, Phys. Rev. B **7**, 743 (1973).

[29] H. Sobotta, H. Neumann, R. Franzheld, and W. Seifert, Phys. Status Solidi B **174**, K57 (1992).

[30] T. Kawashima, H. Yoshikawa, S. Adachi, S. Fuke, and K. Ohtsuka, J. Appl. Phys. **82**, 3528 (1997).

[31] N. A. Sanford, A. V. Davydov, D. V. Tsvetkov, A. V. Dmitriev, S. Keller, U. K. Mishra, S. P. DenBaars, S. S. Park, J. Y. Han, and R. J. Molnar, J. Appl. Phys. **97**, 053512 (2005).

[32] I. V. Kravetsky, I. M. Tiginyanu, R. Hildebrandt, G. Marowsky, D. Pavlidis, A. Eisenbach, and H. L. Hartnagel, Appl. Phys. Lett. **76**, 810 (2000); the values in the table were divided by a factor of 2 in order to get in line with the coefficients definition used in this paper.

[33] I. Loa, S. Gronemeyer, C. Thomson, O. Ambacher, D. Schikora, and D. J. As, J. Raman Spectrosc. **29**, 291 (1998).

[34] F. N. H. Robinson, Phys. Lett. A **26**, 435 (1968).

[35] C.-C. Shih and A. Yariv, Phys. Rev. Lett. **44**, 281 (1980).

[36] C.-C. Shih and A. Yariv, J. Phys. C **15**, 825 (1982).

[37] J. A. Van Vechten, Phys. Rev. **182**, 891 (1969).

[38] G. Irmer, C. Röder, C. Himcinschi, and J. Kortus, Phys. Rev. B **88**, 104303 (2013).